

# Effects of Salts from the Hofmeister Series on the Conformational Stability, Aggregation Propensity, and Local Flexibility of an IgG1 Monoclonal Antibody

Ranajoy Majumdar,<sup>†</sup> Prakash Manikwar,<sup>†,||</sup> John M. Hickey,<sup>†</sup> Hardeep S. Samra,<sup>‡</sup> Hasige A. Sathish,<sup>‡</sup> Steven M. Bishop,<sup>‡</sup> C. Russell Middaugh,<sup>†</sup> David B. Volkin,<sup>\*,†</sup> and David D. Weis<sup>\*,§</sup>

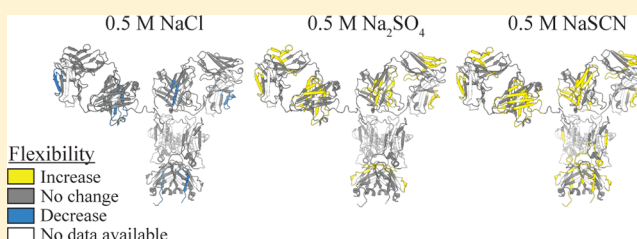
<sup>†</sup>Department of Pharmaceutical Chemistry, Macromolecule and Vaccine Stabilization Center, University of Kansas, Lawrence, Kansas 66047, United States

<sup>‡</sup>Department of Formulation Sciences, MedImmune, One MedImmune Way, Gaithersburg, Maryland 20878, United States

<sup>§</sup>Department of Chemistry and R. N. Adams Institute for Bioanalytical Chemistry, University of Kansas, Lawrence, Kansas 66045, United States

## S Supporting Information

**ABSTRACT:** This work examines the effect of three anions from the Hofmeister series (sulfate, chloride, and thiocyanate) on the conformational stability and aggregation rate of an IgG1 monoclonal antibody (mAb) and corresponding changes in the mAb's backbone flexibility (at pH 6 and 25 °C). Compared to a 0.1 M NaCl control, thiocyanate (0.5 M) decreased the melting temperatures ( $T_m$ ) for three observed conformational transitions within the mAb by 6–9 °C, as measured by differential scanning calorimetry. Thiocyanate also accelerated the rate of monomer loss at 40 °C over 12 months, as monitored by size exclusion chromatography. Backbone flexibility, as measured via H/D exchange mass spectrometry, increased in two segments in the C<sub>H</sub>2 domain with more subtle changes across several additional regions. Chloride (0.5 M) caused slight increases in the  $T_m$  values, small changes in aggregation rate, and minimal yet consistent decreases in flexibility across various domains with larger effects noted within the V<sub>L</sub>, C<sub>H</sub>1, and C<sub>H</sub>3 domains. In contrast, 0.5 M sulfate increased  $T_m$  values, had small stabilizing influences on aggregate formation over time, yet substantially increased the flexibility of two specific regions in the C<sub>H</sub>1 and V<sub>L</sub> domains. While thiocyanate-induced conformational destabilization of the mAb correlated with increased local flexibility of specific regions in the C<sub>H</sub>2 domain (especially residues 241–251 in the heavy chain), the stabilizing anion sulfate did not affect these C<sub>H</sub>2 regions.



Monoclonal antibodies (mAbs) have become successful therapeutic agents because of their high binding specificities for biological targets implicated in a wide range of human diseases. The presence of protein aggregates in therapeutic mAb preparations is of particular concern because of their potential to cause immune responses that may affect the safety or limit the efficacy of therapeutic mAb treatments.<sup>1–3</sup> Antibodies are multidomain, homodimeric proteins with a molecular mass of ~150 kDa, in which the precise value fluctuates because of post-translational modifications such as glycosylation. Their Y-shaped structure can be classified into the antigen binding fragment (F<sub>ab</sub>) and the crystallizable fragment (F<sub>c</sub>) consisting of two heavy (H) and two light (L) chains held together by inter- and intrachain disulfide bonds. The F<sub>ab</sub> and F<sub>c</sub> regions consist of multiple domains. These include the variable (V<sub>L</sub> and V<sub>H</sub>) and constant (C<sub>L</sub>, C<sub>H</sub>1) domains within the F<sub>ab</sub> and the constant domains (C<sub>H</sub>2 and C<sub>H</sub>3) within the F<sub>c</sub>. Antibody structures are further divided into different classes (IgA, IgG, IgM, IgE, and IgD) and subclasses (IgG1, IgG2, IgG3, and IgG4) based on the composition of the constant regions and the number of disulfide bonds.<sup>4</sup>

Antibodies exhibit an array of intrinsic internal motions<sup>5</sup> and can exist as a number of conformers with asymmetric structures that exhibit interdomain flexibility.<sup>6–8</sup> These motions play an important role in their functional activity and biological responses.<sup>9–11</sup> The effect of protein flexibility on overall mAb conformational stability, however, is a more complex relationship and an active area of research.<sup>12,13</sup> Examining the interrelationships between flexibility and stability is especially important not only in helping to design more stable antibodies but also in improving our understanding of how different excipients and salts predispose, initiate, or delay the cascade of events leading to conformational destabilization and aggregation during manufacturing, long-term storage, and administration.<sup>14</sup>

Aggregation of mAbs in solution can occur as a result of covalent or noncovalent protein–protein interactions initiated by changes in pH, temperature, agitation, or interaction with

Received: February 22, 2013

Revised: April 16, 2013

Published: April 17, 2013



solution impurities.<sup>15–18</sup> These interactions occur because of either conformational changes within individual molecules that lead to exposure of nonpolar residues, colloidal effects in solution that alter charge–charge repulsion between molecules, or a combination of both conformational and colloidal effects.<sup>19</sup> In other words, different salts may affect aggregation behavior of mAbs in solution by decreasing conformational stability and/or charge–charge repulsion between two IgG molecules. Protein aggregation has been shown to occur through the formation of partially unfolded monomeric states whose population is minimal under stable solution conditions.<sup>19</sup> With increasing stress, the partially unfolded population increases, leading to subsequent multistep aggregation that results in irreversible loss of protein. For a multidomain protein like an IgG, aggregation-prone segments may also play a key role in the initiation of aggregation<sup>20,21</sup> and in overall antibody instability.<sup>22</sup> The flexibility of the aggregation-prone motifs may change in response to solution conditions or temperature, which may in turn facilitate conformational instability and/or aggregate formation.

Identification of solution conditions that maintain IgG stability and solubility during long-term storage, especially at high protein concentrations, remains a significant challenge in the development of mAbs as biotherapeutics. Salts are generally included in antibody formulations as buffering agents, as well as tonicity and viscosity modifiers.<sup>23</sup> Salts can also affect the solubility and stability of proteins according to their relative position in the Hofmeister series. The Hofmeister series of anions, which have more pronounced effects on protein stability than cations, is as follows:  $\text{SCN}^- > \text{ClO}_4^- > \text{I}^- > \text{ClO}_3^- > \text{Br}^- > \text{NO}_3^- > \text{Cl}^- > \text{CH}_3\text{CO}_2^- > \text{HPO}_4^{2-} > \text{SO}_4^{2-}$ .<sup>24</sup> The members on the left of the series (e.g., thiocyanate, perchlorate, and iodide) are chaotropes that unfold and solubilize proteins. The members on right (e.g., sulfate and phosphate) are kosmotropes that preserve the native structure and decrease solubility, causing proteins to salt out of solution.<sup>25</sup> Chloride is an intermediate member dividing the two groups. The influences of salts on the physical properties of proteins in solution, including melting temperature coefficients,<sup>26</sup> salting-out coefficients,<sup>27</sup> and *B* viscosity coefficients,<sup>28,29</sup> can be ranked according to the positions of the salts in the Hofmeister series, but other properties such as surface tension<sup>29</sup> do not follow the prescribed order. Anions have been found to affect the protein conformational stability<sup>30,31</sup> and rates of aggregation<sup>32,33</sup> in order of their position in the Hofmeister series. A mechanistic explanation of ion effects on protein stability remains an active area of research.<sup>34,35</sup> For example, their influence on protein stability can vary by protein and ion type, as well as by ion concentration and solution pH, by affecting factors such as the water affinity of ions, water structure around proteins, and/or ions interacting directly with protein surfaces.<sup>36–39</sup>

Flexibility is also a crucial consideration for understanding the physicochemical stability of a protein, including its aggregation propensity.<sup>40</sup> Previous work using global measures of dynamics, such as red edge excitation shift fluorescence and high-resolution ultrasonic spectroscopy, has shown that there is a complex relationship between mAb dynamics and aggregation.<sup>14,41,42</sup> However, global approaches cannot be used to assign changes in dynamics to specific regions that contribute to aggregation. Hydrogen/deuterium exchange coupled to mass spectrometry (H/D–MS) can measure backbone flexibility at a resolution of 5–20 residues<sup>43,44</sup> and has been used with mAbs

for biopharmaceutical analysis and comparability studies.<sup>45,46</sup> The effects, on monoclonal antibodies, of methionine oxidation, glycan modification or deglycosylation,<sup>47–49</sup> deamidation and other chemical modifications,<sup>50</sup> and freeze–thaw cycles<sup>51</sup> have all been examined using H/D–MS.

The purpose of this study was to develop a better understanding of the influence of three different anions from the Hofmeister series (sulfate, chloride, and thiocyanate) on the conformational stability, aggregation rate, and polypeptide backbone flexibility of an IgG1 mAb (mAb-B). We have correlated the physical stability changes (measured by DSC and SEC) induced by the anions with changes observed in local backbone flexibility (measured by H/D–MS). In particular, we have identified a potential key role for the local flexibility of two specific segments within the  $\text{C}_{\text{H}2}$  domain in modulating the physical stability of mAb-B.

## ■ EXPERIMENTAL PROCEDURES

**Materials.** Sodium chloride, LC–MS-grade water, acetonitrile, and 2-propanol were obtained from Fisher Scientific (Fair Lawn, NJ). LC-grade acetic acid and phosphoric acid were obtained from Fluka (St. Louis, MO). Formic acid ( $\geq 99\%$  LC–MS-grade) was obtained from Thermo Scientific (Rockford, IL). Porcine pepsin, tris(2-carboxyethyl)phosphine hydrochloride (TCEP), deuterium oxide ( $>99\%$  D), and guanidine hydrochloride were purchased from Sigma-Aldrich (St. Louis, MO). Anhydrous citric acid (99.5%), dibasic anhydrous sodium phosphate, anhydrous sodium sulfate (99%), and sodium thiocyanate ( $>98\%$ ) were purchased from Acros Organics (Fair Lawn, NJ). The IgG1 monoclonal antibody, here termed mAb-B, was formulated at a concentration of 50 mg/mL in 10 mM histidine buffer (pH 6.0) containing 0.005% polysorbate 80.

**Differential Scanning Calorimetry (DSC).** Prior to analysis, mAb-B was diluted to a concentration of 0.5 mg/mL with 20 mM citrate-phosphate (4 mM citrate and 16 mM dibasic sodium phosphate) buffer at pH 6.0 containing NaCl,  $\text{Na}_2\text{SO}_4$ , or NaSCN at concentrations ranging from 0.1 to 1.5 M. DSC was performed using a VP-Capillary differential scanning calorimeter (MicroCal, Northampton, MA). mAb-B samples were analyzed in triplicate over a temperature range of 10–100 °C with a scan rate of 60 °C/h. The data were processed using MicroCal and Origin (OriginLab Ltd.). The data were fit using a multistate model with three transitions. The onset temperature ( $T_{\text{onset}}$ ) of the first transition was taken as the temperature at which the heat capacity exceeded 500 cal  $\text{mol}^{-1}$  °C<sup>–1</sup>.

**Storage Stability and Analysis by Size Exclusion Chromatography (SEC).** mAb-B was diluted to a concentration of 0.5 mg/mL with 20 mM citrate-phosphate (4 mM citrate and 16 mM dibasic sodium phosphate) buffer at pH 6.0 containing either 0.1 M NaCl (control), 0.5 M NaCl, 0.5 M  $\text{Na}_2\text{SO}_4$ , or 0.5 M NaSCN. Aliquots of 0.5 mL of mAb-B were sterilized by being passed through 0.22  $\mu\text{m}$  filters (Millipore, Billerica, MA), dispensed into type I glass vials (West Pharmaceutical Services, Exton, PA) in a sterilized laminar flow hood, stoppered, and stored at four different temperatures (–70, 4, 25, and 40 °C) for a period of up to 12 months. To remove insoluble aggregates, each sample was centrifuged at 14000g for 5 min prior to analysis. SEC was conducted using a 7.8 cm  $\times$  30 cm TSK-Gel BioAssist G3SW<sub>XL</sub> column (TOSOH Biosciences, King of Prussia, PA) at a rate of 0.7 mL/min using a Shimadzu high-performance liquid chromatography (HPLC) system equipped with a photodiode array detector. Gel

filtration standards (Bio-Rad, Hercules, CA) were used for column calibration. The mobile phase was 200 mM sodium phosphate buffer (pH 6.8). The resulting chromatograms were analyzed by integrating the area of the monomer peak detected at 280 nm. The percentage of monomer was measured relative to the total area of all peaks on day 0.

**Deuterated Labeling Buffer Preparation.** The deuterated labeling buffers contained 0.5, 1.0, or 1.5 M salt (sodium chloride, sodium sulfate, or sodium thiocyanate) and 20 mM citrate-phosphate (4 mM citric acid and 16 mM dibasic sodium phosphate) buffer at pH 6.0 in 90 atom % D<sub>2</sub>O. The pH values are reported directly from the pH meter reading without any further correction for the deuterium isotope effect. On the basis of the total volume of H<sub>2</sub>O and D<sub>2</sub>O, the salts, citric acid, and dibasic sodium phosphate were added. The final volume was noted after the pH had been adjusted to 6.0. The final concentrations of the salts were within 3% of their target molarities. The use of 90 atom % D<sub>2</sub>O was adopted here to allow direct comparison with H/D exchange work in a companion study in which some of the buffer components (sucrose and arginine) contributed a non-negligible amount of exchangeable hydrogen to the labeling buffer.<sup>97</sup>

**H/D-MS.** The antibody was diluted to 10 mg/mL in 20 mM citrate-phosphate buffer (4 mM citric acid, 16 mM dibasic sodium phosphate) at pH 6.0. An H/D-X PAL robot (LEAP Technologies, Carrboro, NC) was used for sample preparation and injection. The protein (2  $\mu$ L) was mixed with labeling buffer (38  $\mu$ L) in a 1:20 ratio by volume and incubated at 25 °C for four exchange times (120, 10<sup>3</sup>, 10<sup>4</sup>, and 10<sup>5</sup> s). Three independent replicates of each labeling condition were prepared. Following deuterium labeling, the exchange reaction (40  $\mu$ L) was quenched at 1 °C with 40  $\mu$ L of a 0.5 M TCEP/4 M guanidine hydrochloride/0.2 M sodium phosphate mixture at pH 2.5. Ten microliters of the solution (approximately 16 pmol of mAb-B) was analyzed. Protein stocks and quench buffers were maintained at 1 °C, and the labeling buffers were held at 25 °C using the two temperature-controlled drawers of the H/D-X PAL robot. LC-MS analysis of the deuterated samples was conducted as described previously<sup>52</sup> with the following differences. The refrigerated compartment of the H/D-X PAL robot was used to house the columns, traps, and valves at 1 °C during the course of the experiments. Second, the immobilized pepsin column was back-flushed during the gradient elution step. To minimize carryover, the pepsin column was also washed first with acetonitrile (5%), 2-propanol (5%), and acetic acid (20%) in water and then with 2 M guanidine hydrochloride in 100 mM phosphate buffer (pH 2.5) and after each injection.<sup>52</sup> The typical deuterium recovery achieved with our experimental setup was 60–90% as determined from the deuterium content of fully deuterated model peptides. Data are reported as relative deuterium content levels without correction for back-exchange.

**MS Data Analysis.** A total of 137 peptides covering 85% of the primary sequence of mAb-B were identified using a combination of accurate mass measurement using time-of-flight mass spectrometry and collision-induced dissociation with tandem mass spectrometry on a linear quadrupole ion-trap mass spectrometer (LTQ-XL, Thermo-Scientific) as described previously.<sup>52</sup> A coverage map and a listing of all mapped peptides can be found in the Supporting Information (see Figure S1 and Table S1). H/D exchange data were processed using HDExaminer (Sierra Analytics, Modesto, CA). All mass spectra were manually curated after initial processing. To help

ensure consistency, the charge state for each peptide was kept constant from run to run. To minimize potential biases in data interpretation, each replicate was curated by a different analyst. Most peptide segments were detected in all three replicates, but a smaller number were found in only one or two of the replicates (see Figure S2 of the Supporting Information). An R script, written in house, was used to calculate average deuterium uptake and standard deviations and generate deuterium uptake plots from the exported data. All data with standard deviations exceeding the 95th percentile in the data set were inspected and corrected for data processing errors, if any were found. A statistical analysis of our replicate data, following the method of Houde et al.<sup>45</sup> (see Figures S3 and S4 of the Supporting Information), established the 99% confidence limit for a deuterium uptake difference as  $\pm 0.59$  Da.

**Homology Modeling of mAb-B.** The primary sequences of the heavy and light chains of mAb-B and human IgG1 b12 (Protein Data Bank entry 1HZH)<sup>53</sup> were aligned using CLUSTAL W.<sup>54</sup> The two sequences are approximately 90% homologous, with the most sequence differences in the complementarity-determining region. The primary sequence of mAb-B was threaded onto the 1HZH structure using Discovery Studio 3.0 (Accelrys, San Diego, CA) and renumbered to correct for gaps. The secondary structure of mAb-B was manually reassigned based on the sequence alignment. Models were displayed using Pymol (Schrödinger, LLC, Portland, OR).

## RESULTS

**Effect of Salts on the Conformational Stability of mAb-B.** Representative DSC thermograms showing the thermal transitions of mAb-B in the presence of each of the three salts are shown in Figure 1. The thermal transitions in the DSC thermograms of mAbs have been shown previously to be independent<sup>55,56</sup> and sensitive to changes in pH and ionic strength and to reflect the multistep unfolding of the C<sub>H2</sub>,<sup>57</sup> F<sub>ab</sub>,<sup>58</sup> and F<sub>c</sub><sup>59</sup> domains. For mAb-B formulated in sodium chloride and sodium sulfate, a low-temperature shoulder and two distinct peaks can be seen (Figure 1A,B). DSC analysis of mAb-B in sodium thiocyanate (see Figure 1C) revealed three distinct peaks. The temperatures of the three conformational transitions ( $T_{m1}$ ,  $T_{m2}$ , and  $T_{m3}$ ) at pH 6.0 are listed in Table 1. Thiocyanate (at 0.5 and 1.0 M) had large destabilizing effects on mAb-B as indicated by decreases in the  $T_{m1}$ ,  $T_{m2}$ , and  $T_{m3}$  values compared to control (0.1 M NaCl). In contrast, 0.5 and 1.0 M sulfate increased the three  $T_m$  values of mAb-B. Increasing concentrations of chloride (from 0.1 M to 0.5, 1.0, and 1.5 M) had no notable effect on  $T_{m1}$  but caused small increases in  $T_{m2}$  and  $T_{m3}$ .

The onset temperature,  $T_{onset}$ , was also measured to determine the temperature at which the first observed structural transition within mAb-B began (see Table 1). Chloride, sulfate, and thiocyanate lowered  $T_{onset}$  values compared to the control (0.1 M chloride). The effect of 0.5 and 1.0 M thiocyanate on the  $T_{onset}$  ( $\Delta T_{onset} = -14.9$  and  $-23.8$  °C, respectively) was notably more pronounced than the effect of 0.5 and 1.0 M sulfate ( $\Delta T_{onset} = -2.1$  and  $-1.8$  °C, respectively) and 0.5, 1.0, and 1.5 M chloride ( $\Delta T_{onset} = -3.7$ ,  $-5.7$ , and  $-7.0$  °C, respectively). In summary, at pH 6.0, sulfate and thiocyanate showed opposite effects on the thermal transition temperatures of mAb-B: sulfate stabilized mAb-B, whereas thiocyanate destabilized mAb-B. In addition, all three anions (sulfate,



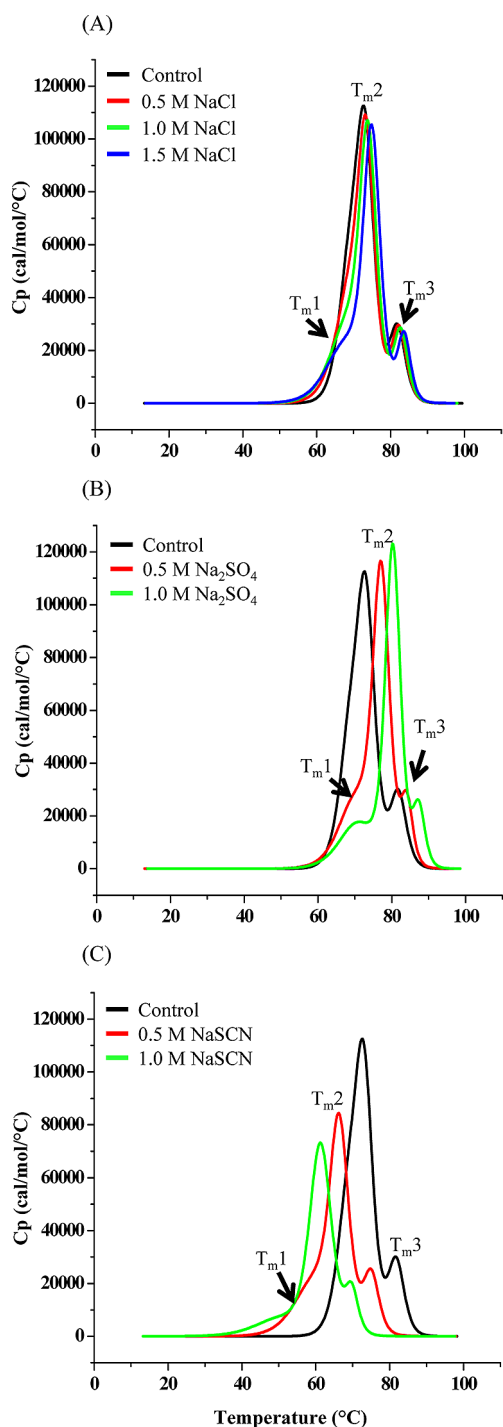


**Figure 1.** Representative DSC thermograms of mAb-B in 20 mM citrate-phosphate buffer (pH 6.0) containing indicated concentrations of different salts. Effect of (A) NaCl, (B) Na<sub>2</sub>SO<sub>4</sub>, and (C) NaSCN on mAb-B conformational stability along with  $T_{m1}$ ,  $T_{m2}$ , and  $T_{m3}$ .

chloride, and thiocyanate) showed titratable effects on the conformational stability of mAb-B.

**Effect of Salts on Aggregation during Storage of mAb-B.** mAb-B samples formulated in a citrate-phosphate buffer containing either 0.1 M sodium chloride, 0.5 M sodium chloride, 0.5 M sodium sulfate, or 0.5 M sodium thiocyanate at pH 6.0 were incubated at various temperatures (−70, 4, 25, and 40 °C) in stoppered glass vials. Individual vials were analyzed by SEC over a period of 12 months. An overlay of

representative chromatograms is shown in Figure 2A. The SEC peaks were assigned as described previously.<sup>60</sup> Initially, there were no differences in the composition of mAb-B in the different formulations compared to the control (Figure 2A, dotted chromatograms). After incubation at 40 °C for 60 days, the amount of soluble monomer decreased, the amount of dimer remained unchanged, and there was an increase in the abundance of fragments (Figure 2A, solid chromatograms). In addition, multimeric aggregates formed in samples of mAb-B containing thiocyanate. Figure 2B shows a plot of the fraction of the soluble monomer (relative to the total peak area at time zero) during its storage for 12 months at different temperatures. It can be seen that mAb-B degraded more rapidly in the presence of thiocyanate and slightly more slowly in the presence of sulfate (up to 12 months), relative to the control at 40 °C. At 4 and 25 °C, the rate of loss of monomer was slower and essentially independent of salt type. Additional time would be required to ascertain if salts cause differences in the aggregation rate at lower temperatures. Interestingly, when frozen (−70 °C), mAb-B samples containing thiocyanate precipitated out of solution, while no differences in the rate of loss of the monomer were observed in samples formulated with sulfate and chloride, especially during multiple freeze–thaw cycles (data not shown).

**Backbone Flexibility of mAb-B in 0.1 M NaCl.** Figure 3 shows representative deuterium uptake curves for six segments from mAb-B, across different IgG1 domains, in 0.1 M sodium chloride (control) and at a concentration of 0.5 M for three different salts. These six uptake curves are representative of the diverse range of H/D exchange kinetics for mAb-B. (Additional deuterium uptake curves for 137 mAb-B segments covering 85% of the total sequence are provided in Figure S5 of the Supporting Information.) The differences can be used to assess relative local backbone flexibility. For example, in the C<sub>H2</sub> domain (heavy chain residues 300–306, peptide 71) deuterium uptake is only apparent after labeling had been conducted for 10<sup>3</sup> s. This high level of protection against deuterium exchange indicates that this part of the C<sub>H2</sub> domain is relatively rigid. In contrast, a region between the V<sub>L</sub> and V<sub>H</sub> domains in the light chain (LC 105–116, peptide 117) was ~75% deuterated within 120 s (relative to the deuterium uptake after incubation for 27 h), indicating that this is a relatively flexible region of mAb-B.

To better define a relative backbone flexibility scale, we used the extent of deuteration at 120 s relative to the theoretical maximal exchange without correction for back-exchange:

$$\text{flexibility (\%)} = \frac{\Delta m_{120\text{ s}}}{Nf} \times 100\% \quad (1)$$

where  $\Delta m_{120\text{ s}}$  denotes the measured mass increase,  $N$  is the number of exchangeable amides, and  $f$  is the mole fraction of deuterium under labeling conditions, here 0.86. The number of exchangeable amides is determined by counting all non-proline residues starting at position 3. (After proteolysis, the first amide becomes a rapidly exchanging amine and the second amide also undergoes rapid back-exchange.<sup>61</sup>) Figure 4A shows the distribution of local flexibility of segments within mAb-B based on this scale. The segments of mAb-B in the lowest quartile on this scale are classified as rigid, segments in the top quartile as flexible, and segments in the middle 50% as intermediate. Figure 4B shows the locations of rigid and flexible segments projected onto a homology model of mAb-B. The H/D exchange measurements show that several loops and  $\beta$ -

**Table 1. Effects of Salt Type and Concentration on Thermal Unfolding Transitions ( $T_m$ ) and Onset of Thermal Unfolding ( $T_{onset}$ ) for mAb-B As Measured by DSC**

[salt] <sup>a</sup>	$T_{onset}$ (°C)			$T_{m1}$ (°C)			$T_{m2}$ (°C)			$T_{m3}$ (°C)		
	mean	SD	$\Delta T_{onset}$	mean	SD	$\Delta T_{m1}$	mean	SD	$\Delta T_{m2}$	mean	SD	$\Delta T_{m3}$
0.1 M NaCl (control)	57.7	0.2	—	69.3	0.1	—	73.6	<0.1	—	82.4	<0.1	—
0.5 M NaCl	54.0	0.2	−3.7	69.5	<0.1	0.3	73.8	<0.1	0.2	82.7	<0.1	0.3
1.0 M NaCl	52.1	0.2	−5.7	69.1	0.2	−0.1	74.7	<0.1	1.1	83.6	<0.1	1.2
1.5 M NaCl	50.7	0.1	−7.0	68.7	0.1	−0.5	75.8	<0.1	2.2	84.7	<0.1	2.3
0.5 M Na <sub>2</sub> SO <sub>4</sub>	55.6	0.7	−2.1	71.1	0.2	1.8	77.7	<0.1	4.1	84.7	<0.1	2.3
1.0 M Na <sub>2</sub> SO <sub>4</sub>	55.9	0.8	−1.8	70.8	0.4	1.5	80.7	<0.1	7.1	87.8	<0.1	5.4
0.5 M NaSCN	42.8	0.5	−14.9	60.3	0.2	−9.0	67.0	<0.1	−6.6	75.8	<0.1	−6.6
1.0 M NaSCN	33.9	0.6	−23.8	51.6	0.5	−17.7	62.2	<0.1	−11.4	70.7	<0.1	−11.7

<sup>a</sup>Samples contained 0.5 mg/mL protein in 20 mM citrate-phosphate buffer (pH 6) with salt as indicated. The mean and standard deviation (SD) are from three separate measurements.

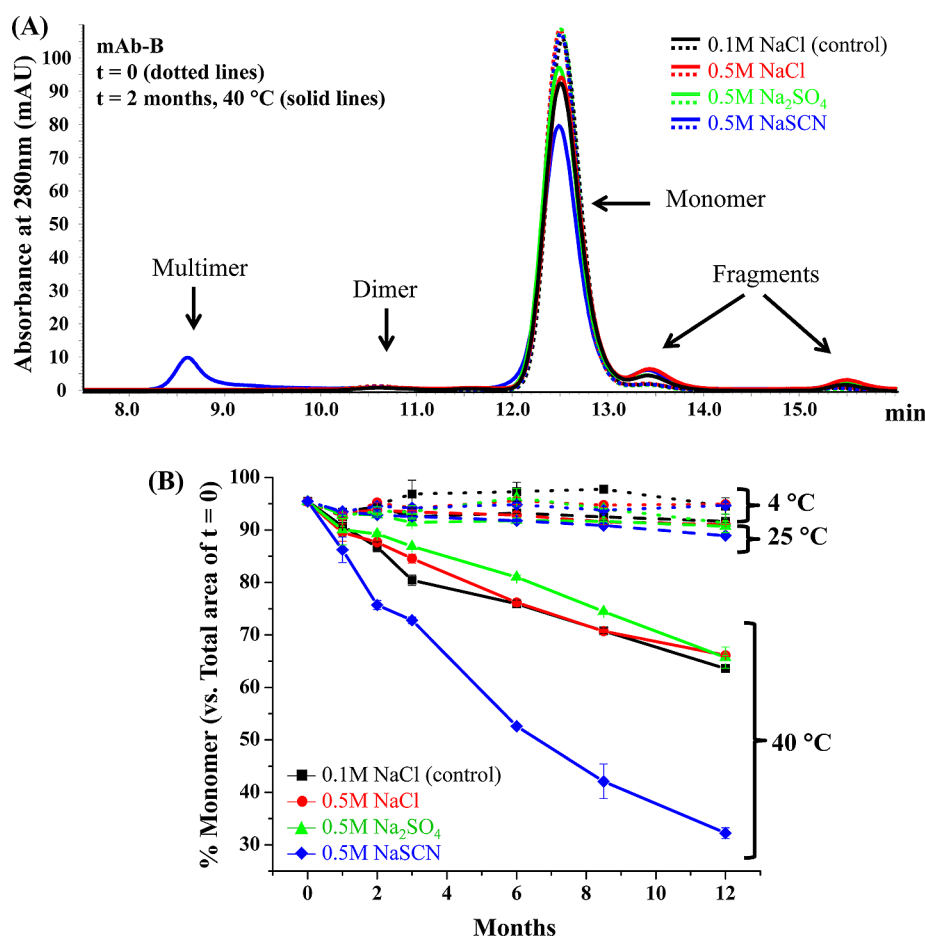


**Figure 2.** mAb-B aggregation during storage at different temperatures as monitored by SE-HPLC. (A) Overlay of SEC chromatograms of mAb-B before and after thermal stress. Dotted lines correspond to mAb-B samples at time zero (no stress), and solid lines correspond to mAb-B samples incubated at 40 °C for 2 months. (B) Effect of salts (NaCl, Na<sub>2</sub>SO<sub>4</sub>, and NaSCN) and thermal stress (4, 25, and 40 °C) on mAb-B monomer loss. Data were collected in duplicate on days 0, 28, 60, 90, 180, 260, and 360. Samples of mAb-B were prepared in 20 mM citrate-phosphate buffer (pH 6.0) with either 0.1 M NaCl (control, black trace), 0.5 M NaCl (red trace), 0.5 M Na<sub>2</sub>SO<sub>4</sub> (green trace), or 0.5 M NaSCN (blue trace).

strands on the surface of the F<sub>ab</sub> region and C<sub>H</sub>3 domain are relatively flexible (yellow segments). Most regions within the C<sub>H</sub>2 domain as well as some buried  $\beta$ -strands and loops in other domains of mAb-B are relatively rigid (blue segments). As described in other studies,<sup>62–64</sup> we found no strong correlation between the mAb-B flexibilities, measured in solution, and segment-averaged *B* factor values from the crystal structure of 1HZH<sup>53</sup> for 22 peptides with identical sequences from the constant domains of the two IgG1s (data not shown).

**Identifying the Effects of Salts on the Local Backbone Flexibility of mAb-B.** In addition to providing information about the relative local flexibility of mAb-B in 0.1 M NaCl, we can identify regions that undergo changes in H/D exchange kinetics in response to changes in salt type or concentration. The representative H/D exchange data in Figure 3 show some of the effects of the three different salts, at 0.5 M, on the local flexibility of mAb-B. For each region, there was an increase or decrease in the level of deuterium uptake at one or more of the

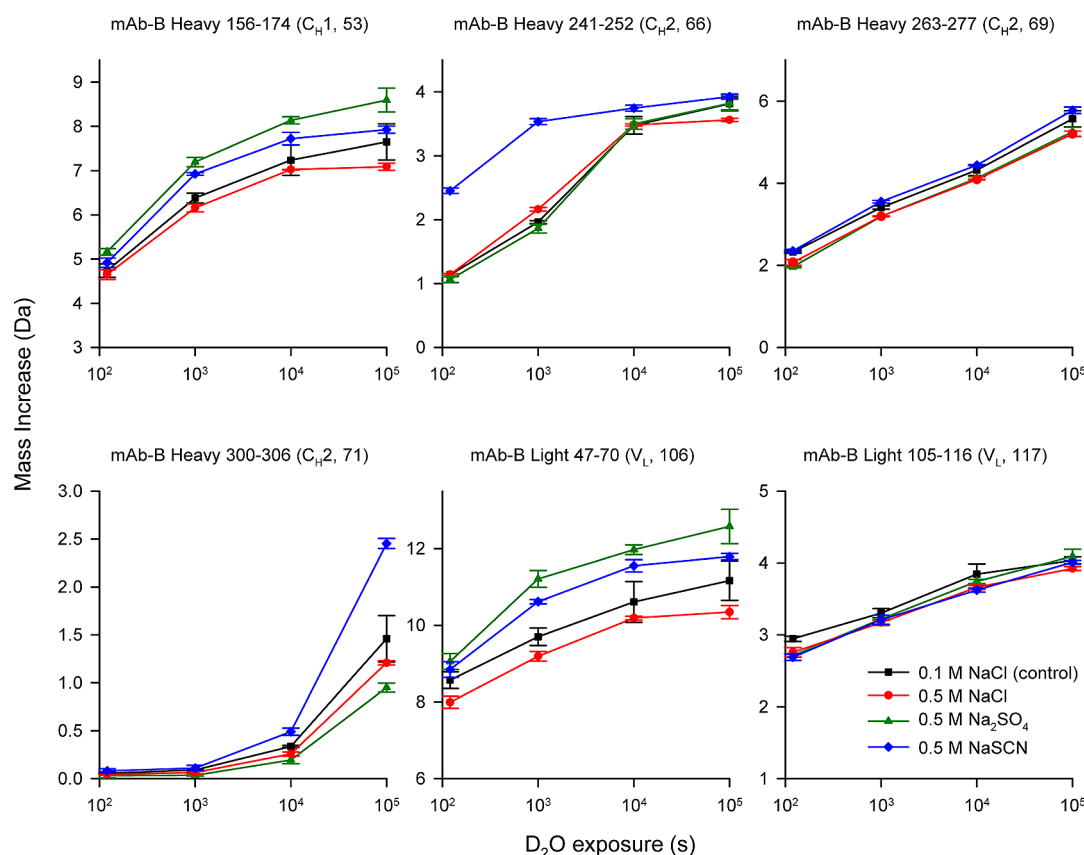


**Figure 3.** Effect of different salts on the deuterium uptake in six segments from different domains of mAb-B. The error bars denote one standard deviation.

exchange times; however, not all of these differences exceeded the 99% confidence limit of  $\pm 0.59$  Da. These individual curves provided a visual representation of salt effects on deuterium uptake for the individual segments. To obtain a more quantitative and global view of salt-induced changes in deuterium uptake, individual differences in deuterium uptake, i.e.,  $\Delta\Delta m(t) = \Delta m_{\text{salt}}(t) - \Delta m_{\text{control}}(t)$ , for every peptide at every labeling time are plotted in Figure 5. This figure shows both the magnitudes and signs of the differences and whether the differences exceeded the 99% confidence level for significance. Positive values indicate segments in which flexibility increased relative to the 0.1 M NaCl control, while negative values indicate a decrease in flexibility. In Figure 5, the horizontal axis arranges the peptides in order from the N-terminal end of the heavy chain to the C-terminal end of the light chain, similar to the plots described by Houde et al.<sup>47</sup> The domain location for each peptide is denoted by the shading. Mass differences exceeding statistical significance at the 99% confidence level [ $|\Delta\Delta m| \geq 0.59$  Da (see Experimental Procedures and Figures S2–S4 of the Supporting Information)] are indicated by the dashed horizontal lines. mAb-B regions that experienced significant changes in deuterium uptake in the presence of 0.5 M chloride, sulfate, and thiocyanate at one or more deuterium exchange times compared to the 0.1 M NaCl control are mapped onto a homology model of mAb-B in Figure 6. Regions that showed increases in flexibility (positive values in Figure 5) are colored yellow; decreases in flexibility (negative values in Figure 5) are colored blue. Unaffected regions are colored gray, and regions without H/D exchange data are colored white.

**Effects of 0.5 M Chloride.** For the six representative peptide segments shown in Figure 3, the only significant effect of chloride at 0.5 M was in the light chain 47–70 segment, located in the  $V_L$  domain of mAb-B (peptides 106–108 in Figure 5), which experienced an increased level of protection against H/D exchange. For the other five segments shown in Figure 3, chloride had no significant effect on deuterium uptake relative to the control. Figures 5 and 6 show the effect of 0.5 M chloride across the entire mAb molecule. The addition of 0.5 M chloride caused only a few significant changes in the local flexibility of mAb-B compared to the 0.1 M chloride control. In addition to the  $V_L$  segment (47–70), there were also decreases in flexibility in the HC 124–147 segment (peptide 51) in the  $C_H1$  domain and the HC 424–446 segment (peptide 94) in the  $C_H3$  domain. Interestingly, there was an overall trend of decreased flexibility across mAb-B (defined by slower deuterium uptake for most segments in Figure 5) in the presence of 0.5 M chloride, but most of the individual differences were not significant at the 99% confidence level.

**Effects of 0.5 M Sulfate.** Sulfate caused localized changes in the flexibility of mAb-B as summarized in Figure 6. For example, data in Figures 3 and 5 show that 0.5 M sulfate caused substantial increases in the level of deuterium uptake in the  $C_H1$  domain (HC 156–174 in Figure 3; peptides 51–53 in Figure 5) and in the  $V_L$  domain (LC 47–70 in Figure 3; peptides 106–108 in Figure 5). In addition to these increases, several other segments (HC 37–80 corresponding to peptides 11, 22, 23, 30, and 35; HC 380–404 corresponding to peptides 83–85 and 87; and LC 136–161 corresponding to peptide 126) exchanged slightly faster than the control.

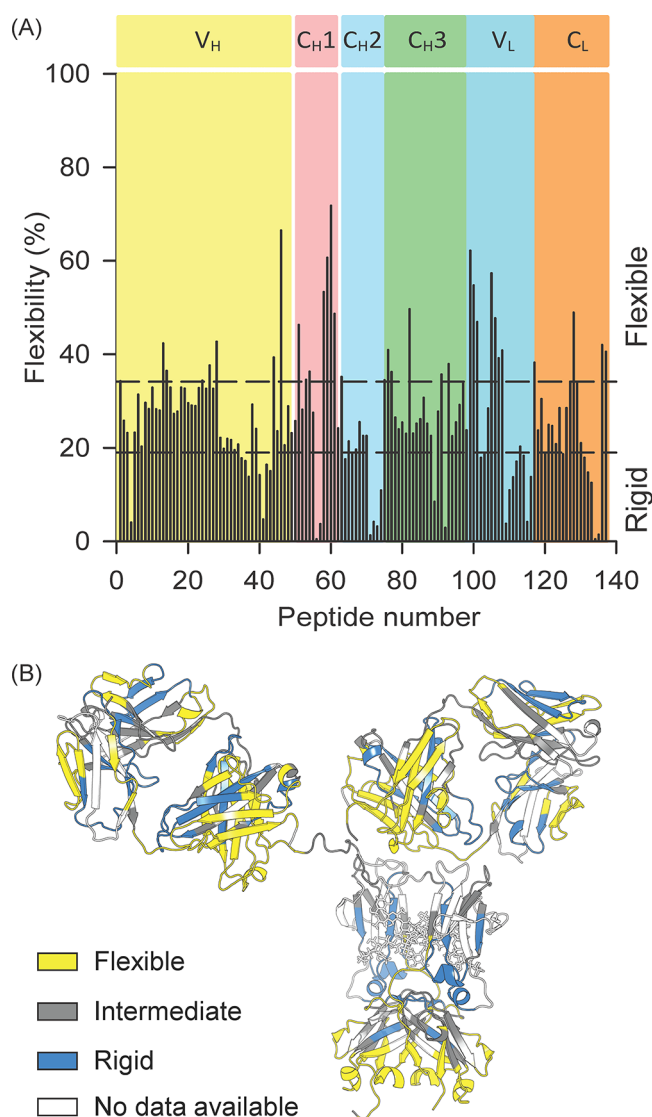


**Figure 4.** Local flexibility of mAb-B, as measured by H/D exchange in 0.1 M NaCl at pH 6.0. (A) Flexibility, as obtained from the ratio of the extent of deuteration at 120 s relative to the theoretical maximal exchange without correction for back-exchange (eq 1). Colors denote the different domain boundaries. The dashed lines denote the top and bottom quartiles. The maximal flexibility is 85.5%. (B) Flexibility data plotted on a homology model of mAb-B. Peptides representing the bottom quartile are classified as rigid (blue), peptides representing the middle 50% as intermediate (gray), and peptides representing the top quartile as flexible (yellow). Regions without H/D exchange data are colored white. In cases where overlapping segments had different flexibility categories, flexible and rigid categories took priority over the intermediate category, and the rigid category took priority over the flexible category (five amino acids only).

**Effects of 0.5 M Thiocyanate.** Thiocyanate caused substantial increases in the level of deuterium uptake in two different segments of the C<sub>H</sub>2 domain, as summarized in Figure 6. Exchange was faster in the HC 241–252 region (120 and 10<sup>3</sup> s in Figure 3; also see peptides 64–68 in Figure 5). In addition, the HC 300–306 region also exchanged more quickly, but this increase in the level of deuterium uptake was only evident at the longest exchange time, 10<sup>5</sup> s (see Figure 3; see also peptides 71–73 in Figure 5). Figure 5 shows that several additional regions in the heavy chain (peptides HC 37–59, 61–80, 124–

147, 198–220, 334–348, 382–398, and 429–446) and light chain (peptides LC 47–70, 136–161, and 186–212) in mAb-B, corresponding to peptides 11, 29, 30, 51, 61, 75, 86, 95, 106, 107, 126, 136, and 137 exchanged faster than the control.

**Overlapping Effects of Anions.** For a few of the peptide segments of mAb-B, the three anions had more complex effects on the deuterium exchange kinetics. For example, sulfate and thiocyanate accelerated both HC 124–147 in the C<sub>H</sub>1 domain (peptide 51) and LC 47–70 in the V<sub>L</sub> domain (peptide 106), while chloride slowed H/D exchange (see Figure 5). Similarly, both sulfate and thiocyanate accelerated exchange in HC 37–59 in the V<sub>H</sub> domain (peptide 11) and HC 382–398 in the C<sub>H</sub>3 domain (peptide 86). Finally, 0.5 M chloride and thiocyanate caused opposite effects on deuterium uptake in the HC 429–446 segment of the C<sub>H</sub>3 domain corresponding to peptide 95 (see Figure 5 and Table S1 of the Supporting Information).

**Effects of Salt Concentration on the Local Flexibility of mAb-B.** The H/D exchange experiments at 25 °C show that the three salts at 0.5 M have localized effects on the flexibility of mAb-B. To determine if the magnitudes of these local effects were concentration-dependent, we measured H/D exchange after labeling had been conducted for 10<sup>3</sup> s for mAb-B in 1.0 and 1.5 M sodium chloride as well as in 1.0 M sodium sulfate and 1.0 M sodium thiocyanate. A minimized set of 43 mAb-B segments was selected for analysis. This set represented all domains of mAb-B and consisted of both regions that were and were not affected by 0.5 M salts. No significant differences in H/D exchange were noted for any of these 43 segments in 1.0 M salts compared to 0.5 M salts (plots of deuterium uptake vs salt concentration for each segment are shown in Figure S6 of the Supporting Information). These results show that changes in local flexibility of mAb-B do not titrate to any appreciable extent beyond 0.5 M salt, at least in the citrate-phosphate buffer (pH 6.0) employed in these experiments. Because an increased ionic strength with 1.0 or 1.5 M chloride did not have any further significant effect on the local flexibility of the mAb, the changes observed with sulfate were not due to changes in ionic strength differences but rather are due to the anion. Moreover, because the majority of mAb-B segments do not show any perturbation of flexibility in the presence of the different salts (see Figure S6 of the Supporting Information), intrinsic exchange rates of various mAb-B segments were not substantially altered by changes in salt types or ionic strength conditions.

## DISCUSSION

The purpose of this work was to probe the effects of anions from the extremes of the Hofmeister series on the local flexibility of various domains of an IgG1 mAb and examine these results in the context of conformational stability and aggregation propensity. Thiocyanate, an extreme chaotrope, decreased mAb-B's thermal stability, as indicated by DSC, and accelerated aggregation, as measured by SEC. Sulfate, an extreme kosmotrope, had the opposite effects. Chloride, positioned in the middle of the Hofmeister series, had minor effects on both the thermal and the physical stability of mAb-B. In contrast, the effects of the anions on local flexibility, as revealed by H/D exchange, were more complex (see Figures 5 and 6). Sodium chloride induced a small but nearly global decrease in flexibility, although most changes in individual peptide segments were not statistically significant. While thiocyanate and sulfate had opposing effects on physical

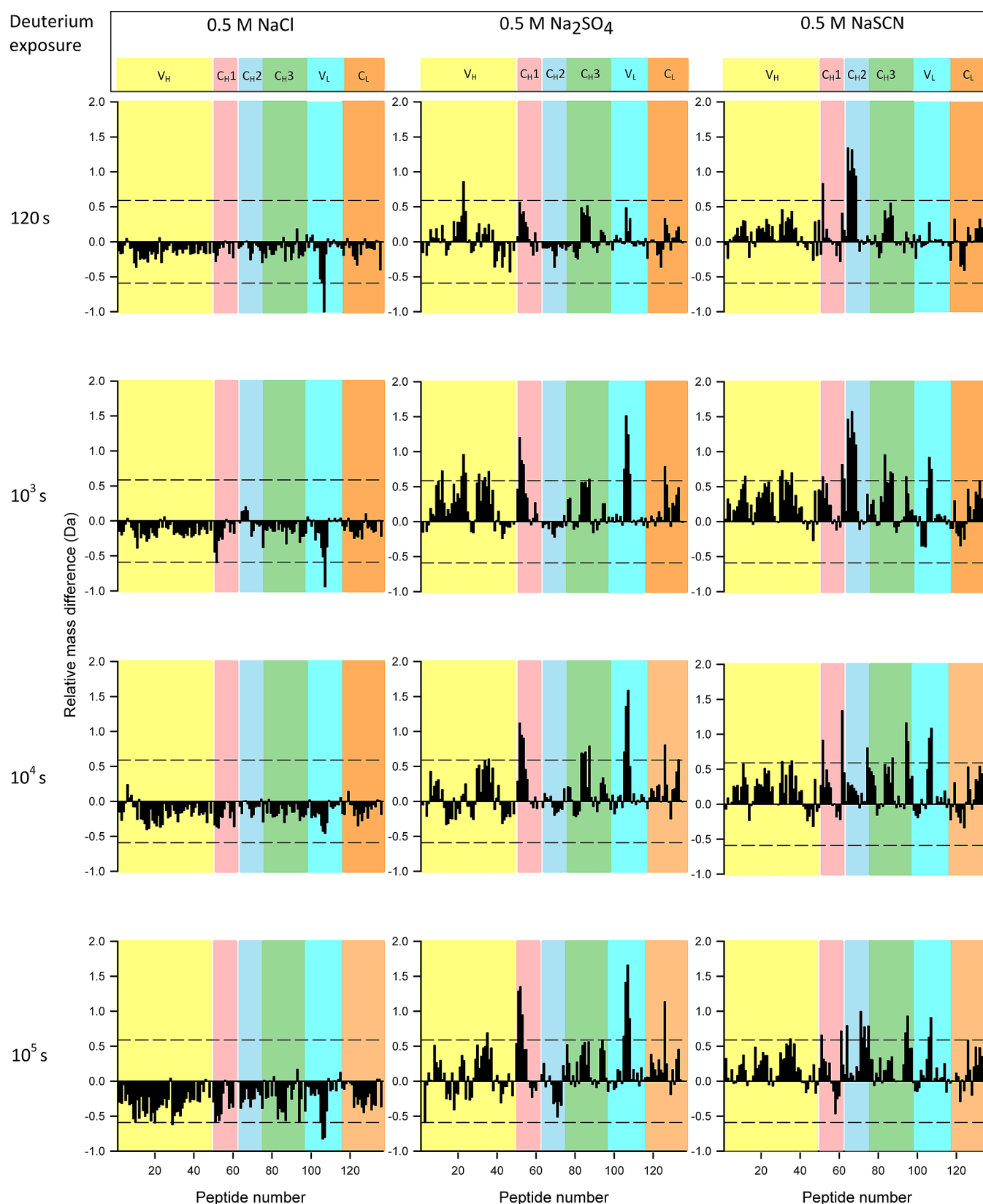


**Figure 5.** Relative deuterium uptake differences for all 137 segments of mAb-B in the presence of 0.5 M salts relative to the control solution (0.1 M sodium chloride) as measured by H/D-MS at each deuterium exposure time. The dashed lines at  $\pm 0.59$  Da represent the 99% confidence limit for the mass difference values. The horizontal axis denotes the ordinal peptide numbers, which are sorted in ascending order based on the midpoint of their sequences. Colors denote the different domain boundaries. Positive vertical values in these plots denote increased flexibility in the particular segment in the presence of the particular salt compared to the control (0.1 M sodium chloride), and negative vertical values denote decreased flexibility. Locations of the mAb domains shown in the figure are only approximate because some peptide segments span two different domains. See Table S1 of the Supporting Information for the locations of the peptides in the mAb-B sequence.



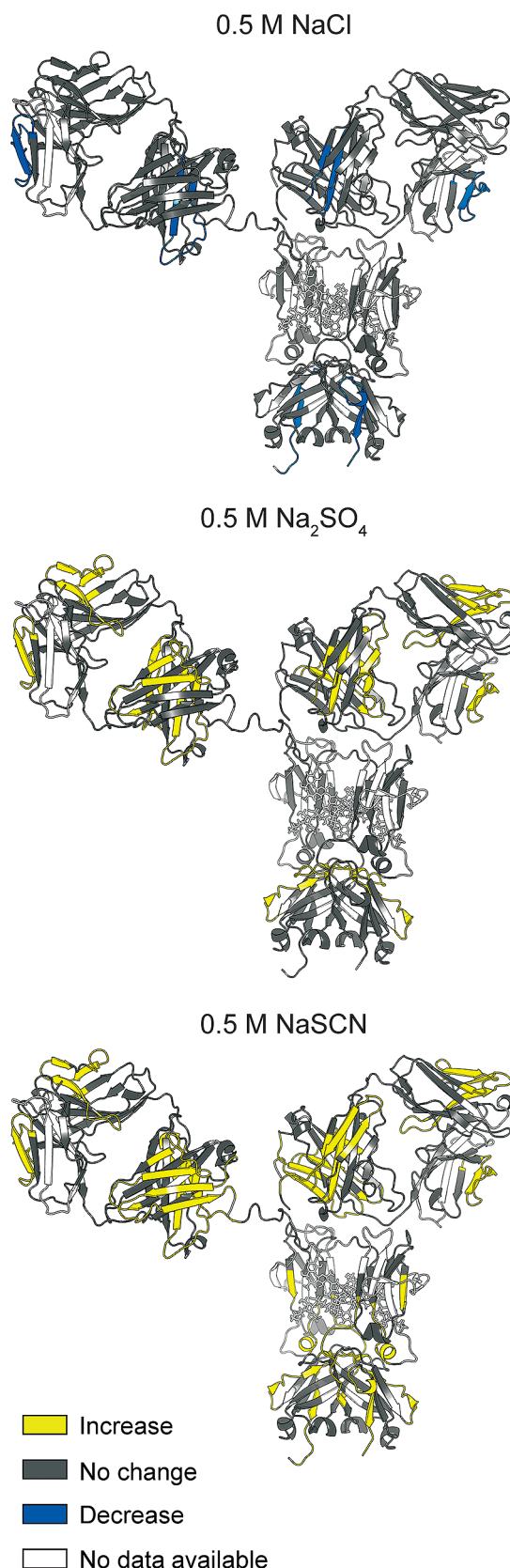


**Figure 6.** Effects of salts on the flexibility of mAb-B relative to the control (0.1 M sodium chloride), as measured by H/D–MS plotted onto a homology model of mAb-B. Changes in flexibility are colored according to the legend.

stability, both anions increased the local flexibility in mAb-B. The increases in flexibility were not global; many regions of mAb-B were unaffected by either anion. While thiocyanate and sulfate had similar effects on many regions of mAb-B, notably in the  $C_H1$  and  $V_L$  domains, there were notable differences in the  $C_H2$  domain, where thiocyanate increased flexibility but sulfate had no effect. We will return to the significance of these findings to the mechanisms by which anions alter physical stability below. First, we address the issue of how these anions might directly alter the kinetics of H/D exchange.

Salts might alter the kinetics of H/D exchange by changing the protein or by changing the chemical exchange process. According to the Linderström–Lang mechanism in the usual EX2 limit, the rate of H/D exchange depends on both flexibility ( $k_{cl}/k_{op}$ ) and intrinsic chemical exchange ( $k_{int}$ ).<sup>65,66</sup>

$$\text{NH(closed)} \xrightleftharpoons[k_{cl}]{k_{op}} \text{NH(open)} \xrightarrow{k_{int}} \text{ND}$$

$$k_{\text{obs}} = \frac{k_{op}}{k_{cl}} k_{\text{int}}$$

Changes in intrinsic exchange would lead to altered H/D exchange kinetics even if the flexibility of mAb-B was not affected. While base-catalyzed exchange in poly-DL-arginine is highly sensitive to changes in ionic strength,<sup>67</sup> charged side chains exhibit an only moderate ionic strength dependence in more realistic peptide models.<sup>68</sup> Similarly, changes in ionic strength have only very modest effects on intrinsic exchange by amides in alanine model peptides.<sup>61</sup> Increasing the concentration of NaCl from 0.1 to 1.5 M and those of  $\text{Na}_2\text{SO}_4$  and NaSCN from 0.5 to 1.0 M in our work with mAb-B did not result in any significant changes in H/D exchange kinetics (see Figure S6 of the Supporting Information). Although sulfate was shown to slow and thiocyanate to increase intrinsic exchange in *N*-acetylalanine at pH 4,<sup>69</sup> in our work we found that H/D exchange was not significantly affected by salts in the large majority of peptide segments at pH 6.0. On the whole, we conclude that these anions do not have substantial effects on intrinsic exchange in mAb-B. Thus, we attribute the observed effects, instead, to the influence of the anions on the backbone flexibility of mAb-B.

The pattern of backbone flexibility of mAb-B at pH 6.0, as reported by H/D exchange at 120 s (see Figure 4), is consistent with several other H/D exchange studies of IgG1 monoclonal antibodies.<sup>47–51</sup> We note, in particular, the HC 241–252 (peptide 65, FLFPPKPKDTL) and HC 300–306 (peptide 71, YRVSVSL) segments, both found in the  $C_H2$  domain, which we have found to be thiocyanate-sensitive. H/D exchange kinetic data are available for both of these segments in two previous studies<sup>47,49</sup> and for HC 241–252 in two others<sup>50,70</sup> (the sequence numberings are offset slightly). In all of these other works, HC 241–252 exchanges with an approximate midpoint of  $\sim 10^3$  s. All of the uptake data, when plotted on a logarithmic scale, have the same sigmoidal profile. In the case of HC 300–306, no deuterium uptake was observed because the maximal level of labeling in previous work was only  $3 \times 10^4$  s; in our study, we were able to detect H/D exchange by extending the  $\text{D}_2\text{O}$  exposure to  $10^5$  s. The consistency in these results in the  $C_H2$  domain is a testament to the intralaboratory repeatability of H/D exchange measurements on mAbs.

Although direct, quantitative comparisons are impeded by slight differences in peptide coverage and labeling conditions,

domain-scale qualitative comparisons can still be drawn. On a domain-by-domain basis, our H/D exchange data for mAb-B are in good agreement with previous work. What emerges is a general picture of backbone flexibility in the conserved regions of IgG1 mAbs, validated across several different IgG1s examined in different laboratories. We find that the C<sub>H</sub>1 and C<sub>H</sub>3 domains are relatively more dynamic while the C<sub>H</sub>2 domain is the most rigid. (In one of these works,<sup>47</sup> exchange in the C<sub>H</sub>2 domain appears to be more protected, but this is probably because maximal exchange was limited to 240 min.)

In comparison to the 0.1 M NaCl control, 0.5 M NaCl caused only small changes in the thermal melting (Figure 1). Aggregation kinetics, as measured by the loss of monomer, were similar in 0.1 and 0.5 M NaCl at 4, 25, and 40 °C over 12 months (Figure 2); 0.5 M NaCl caused only a few significant decreases in local flexibility in the C<sub>H</sub>1, V<sub>L</sub>, and C<sub>H</sub>3 domains of mAb-B, along with an overall trend toward reduced flexibility across the molecule (Figure 5). This overall trend is interesting, although it must be noted that most of these effects are not greater than the statistically significant cutoff of 99% confidence (Figure 5). Chloride anions decreased the local flexibility of EnvZ, an osmolality-sensing inner membrane histidine kinase, but the effect was attributed to a change in solution osmolality.<sup>71</sup> Chloride–protein interactions can occur via weak binding of chloride to protein surface residues either through electrostatic or through nonspecific interactions.<sup>72</sup> For example, the aggregation propensity of three different monoclonal antibodies correlated directly with decreases in their net charge (reduced valence) and the apparent *T*<sub>m</sub>1 at low salt chloride concentrations (0–160 mM).<sup>73</sup>

Sulfate anions increased the *T*<sub>m</sub> values of all three thermal transitions of mAb-B, with the largest increase being observed for *T*<sub>m</sub>2, corresponding to melting of the F<sub>ab</sub> region<sup>74</sup> (Figure 1). In the accelerated storage stability studies, 0.5 M Na<sub>2</sub>SO<sub>4</sub> protected mAb-B against aggregation to a small extent at 40 °C during the 12 month storage (Figure 2), with less differences noted at the end. Concomitantly, substantial increases in flexibility were observed in two segments of the C<sub>H</sub>1 and V<sub>L</sub> domains along with more subtle increases in flexibility in certain regions of the V<sub>H</sub>, C<sub>H</sub>1, and C<sub>H</sub>3 domains (Figures 5 and 6). Stabilizing effects of sulfate on other proteins<sup>75</sup> have been proposed to occur by stabilization of the native folded state,<sup>76,77</sup> by the binding of sulfate to positively charged residues,<sup>72,76,78,79</sup> or by the increased level of hydration arising from a higher number of dipoles on protein surfaces.<sup>80</sup> Sulfate anions, however, also increase the surface tension of aqueous solutions<sup>29,81–83</sup> with increasing concentrations leading to higher protein surface energies (salting-out activity) that may accelerate protein aggregation.<sup>37,84</sup> Sulfate can also overcharge proteins, leading to the increased local flexibility of the C<sub>H</sub>1 and V<sub>L</sub> domains via charge repulsion between bound sulfate anions.<sup>38</sup> The interplay of these competing phenomena gives rise to the intriguing effects of sulfate anions on the stability and solubility of different proteins.<sup>76,81,85,86</sup> The effect of sulfate anions on stabilizing mAb-B in terms of conformational stability, and to a lesser extent against aggregation over time, combined with increases in local flexibility in two segments of the C<sub>H</sub>1 and V<sub>L</sub> domains, highlights the complex interrelationships between protein stability and flexibility.<sup>40</sup>

Thiocyanate anions substantially destabilized mAb-B. The largest effect of thiocyanate was on *T*<sub>m</sub>1 (Figure 1), corresponding to the unfolding of the C<sub>H</sub>2 domain.<sup>74</sup> Thiocyanate also dramatically increased the level of aggrega-

tion, as measured by monomer loss, at 40 °C over a 12 month period (Figure 2). In contrast to sulfate or chloride, only thiocyanate caused substantial increases in local flexibility in two separate segments of the C<sub>H</sub>2 domain (Figures 3 and 6). The mechanism of thiocyanate-induced protein destabilization is thought to involve its interaction with both positively charged residues and apolar hydrophobic regions on the surface of either native proteins or partially unfolded intermediates,<sup>87–90</sup> thereby decreasing the overall charge on the protein and weakening the electrostatic repulsion<sup>91,92</sup> leading to enhanced protein–protein interactions<sup>93–95</sup> resulting in aggregation. The destabilizing effects of thiocyanate on protein flexibility are not necessarily observed with all proteins. In the case of recombinant  $\gamma$ -interferon, no notable differences in H/D exchange kinetics were observed in 0.3 M KSCN versus KCl, although the two salts had different effects on this protein's solubility and aggregation.<sup>96</sup> In addition to effects on the C<sub>H</sub>2 domain of mAb-B, additional subtle increases in local flexibility were observed across mAb-B (Figure 5), indicating thiocyanate may have specific weaker interactions with several other segments throughout the mAb. These results also correlate with the decrease in the conformational stability of mAb-B as observed for *T*<sub>m</sub>2 (F<sub>ab</sub> region) and *T*<sub>m</sub>3 (C<sub>H</sub>3 domain) caused by thiocyanate.

The increase in the local flexibility (HC 241–252 and 300–306) of the C<sub>H</sub>2 domain of mAb-B in the presence of thiocyanate correlates with conformational destabilization of the C<sub>H</sub>2 domain (*T*<sub>m</sub>1) and accelerated aggregation during storage. Similar effects were observed in a separate study in our laboratories where arginine hydrochloride also destabilized mAb-B and increased the flexibility of the HC 241–252 segment in the C<sub>H</sub>2 domain.<sup>97</sup> At the same time, stabilizing additives had no effect on these two regions within the C<sub>H</sub>2 domain (NaCl and Na<sub>2</sub>SO<sub>4</sub> in this work and sucrose in our companion study). These observations lead to the conclusion that the flexibility of HC 241–252 and 300–306 regions in the C<sub>H</sub>2 domain is an important factor in maintaining the overall physical stability of mAb-B. We also observed increases in flexibility in the N-terminal region of the C<sub>H</sub>3 domain (HC 379–398, peptide 83). All of these observations are consistent with increases in the flexibility in the C<sub>H</sub>2 and C<sub>H</sub>3 domains of other IgG1 mAbs caused by glycan modifications<sup>47,48</sup> and methionine oxidation.<sup>48,49</sup> Whether these changes merely correlate with a loss of stability or actually cause the destabilization cannot be determined simply on the basis of the H/D exchange measurements. However, several additional pieces of evidence suggest that the C<sub>H</sub>2 domain plays a causal role in aggregation. Agitation-induced aggregation of an F<sub>c</sub> fragment was inhibited by the binding of protein A and protein A-derived peptides.<sup>98</sup> Because protein A binds to several residues from the C<sub>H</sub>2 and C<sub>H</sub>3 domains of an IgG protein, these results further support the idea that the C<sub>H</sub>2 region is important in mediating IgG aggregation. In a separate study, an isolated C<sub>H</sub>2 domain was stabilized by engineering an L242C/K334C double mutant that introduced a stabilizing disulfide bond.<sup>99</sup> This disulfide bond presumably decreased the flexibility of the HC 241–251 region. Hence our results, with an intact IgG1 mAb, further highlight the importance of the HC 241–251 segment of the C<sub>H</sub>2 domain in the physical stability of IgG1 mAbs.

On the other hand, both sulfate and thiocyanate increased the local flexibility in small regions of both the F<sub>ab</sub> and C<sub>H</sub>3 domains while chloride decreased flexibility in these same

regions (see Figure 6). These changes in local flexibility in mAb-B do not correlate with conformational stability or the aggregation propensity of mAb-B. These results highlight once again the complex interrelationships between protein flexibility and stability<sup>40</sup> as well as the need for local measurements of dynamics. Global measurements of dynamics of a mAb may be less informative than local measurements because not all increases in flexibility result in decreases in stability. Here, the overall change in dynamics would depend on the balance of effects between the relatively flexible  $F_{ab}$  and  $C_{H3}$  domains and the comparatively rigid  $C_{H2}$  domain (Figure 4).

Identification of backbone flexibility changes in specific regions within an IgG1 mAb that respond to changes in solution conditions (e.g., the presence of various additives) and correlation of these changes with conformational stability and physical stability during long-term storage should provide better mechanistic insight into stabilization and formulation development of antibody-based drugs. H/D-MS measurements could complement high-resolution theoretical approaches for predicting the stability of proteins based on salt-protein interactions.<sup>31,100</sup> For example, the salt-induced effects observed in this work were localized to short segments of the mAb-B backbone. Hence, H/D-MS experiments could be designed to screen specific regions of a mAb for the effects of different additives to better predict their effects on physical stability. It remains to be seen whether the correlations between flexibility and stability persist across different subclasses (e.g., IgG1, IgG2, and IgG4) or different classes of mAbs (IgG, IgM, and IgA). Finally, computational studies mapping electrostatic potentials on the surface of the antibody at a specific pH and in the presence of various salts may help to further explain the molecular mechanism of anion-induced changes in local flexibility observed in this study.<sup>101–103</sup>

## ■ ASSOCIATED CONTENT

### ■ Supporting Information

A statistical analysis of the reproducibility of our H/D-MS measurements (text), the primary sequence coverage map for 137 peptides from mAb-B (Figure S1), the distribution of replicates used in this study (Figure S2), a histogram showing the reproducibility of H/D-MS results (Figure S3), the distribution of standard deviations with respect to the number of exchangeable hydrogens in peptides (Figure S4), deuterium uptake curves for all segments from mAb-B in formulations containing 0.5 M chloride, sulfate, and thiocyanate compared to the control (0.1 M chloride) (Figure S5), plots of deuterium uptake versus salt concentration for 43 selected peptides from mAb-B (Figure S6), and the ordinal peptide numbers and their locations in the mAb-B sequence (Table S1). This material is available free of charge via the Internet at <http://pubs.acs.org>.

## ■ AUTHOR INFORMATION

### Corresponding Author

\*D.B.V.: e-mail, [volkin@ku.edu](mailto:volkin@ku.edu); phone, (785) 864-6262.  
D.D.W.: e-mail, [dweis@ku.edu](mailto:dweis@ku.edu); phone, (785) 864-1377.

### Present Address

<sup>†</sup>Department of Formulation Sciences, MedImmune, One MedImmune Way, Gaithersburg, MD 20878.

### Author Contributions

R.M. and P.M. contributed equally to this work.

## Funding

We acknowledge financial support from MedImmune and the Kansas Bioscience Authority.

## Notes

H.S.S., H.A.S., and S.M.B. are employees of MedImmune, LLC.

## ■ ACKNOWLEDGMENTS

We acknowledge Dr. Jianwen Fang and Dr. Yaping Fang of the Applied Bioinformatics Laboratory at the University of Kansas for developing the R script to generate deuterium uptake curves.

## ■ ABBREVIATIONS

DSC, differential scanning calorimetry;  $T_m$ , midpoint of the thermal melting curve by DSC;  $T_{onset}$ , onset of thermal unfolding by DSC; mAb, monoclonal antibody;  $C_{H1}$ – $C_{H3}$ , constant domains 1–3, respectively, of the heavy chain of a monoclonal antibody;  $V_H$ , variable domain of the heavy chain of a monoclonal antibody;  $V_L$ , variable domain of the light chain of a monoclonal antibody;  $F_{ab}$ , fragment, antigen binding region of a monoclonal antibody;  $F_c$ , fragment, crystallizable region of a monoclonal antibody; HC, heavy chain of a monoclonal antibody; LC, light chain of a monoclonal antibody; LC-MS, liquid chromatography-mass spectrometry; H/D-MS, hydrogen/deuterium exchange with mass spectrometry; SEC, size exclusion chromatography.

## ■ REFERENCES

- (1) Rosenberg, A. S. (2006) Effects of protein aggregates: An immunologic perspective. *AAPS J.* 8, E501–E507.
- (2) Wang, W., Singh, S. K., Li, N., Toler, M. R., King, K. R., and Nema, S. (2012) Immunogenicity of protein aggregates: Concerns and realities. *Int. J. Pharm.* 431, 1–11.
- (3) Filipe, V., Jiskoot, W., Basmeleh, A. H., Halim, A., and Schellekens, H. (2012) Immunogenicity of different stressed IgG monoclonal antibody formulations in immune tolerant transgenic mice. *mAbs* 4, 740–752.
- (4) Janeway, C., Travers, P., Walport, M., and Shlomchik, M. J. (2001) *Immunobiology*, 5th ed., Garland Publishing, New York.
- (5) Roux, K. H., Strelets, L., and Michaelsen, T. E. (1997) Flexibility of human IgG subclasses. *J. Immunol.* 159, 3372–3382.
- (6) Saphire, E. O., Stanfield, R. L., Max Crispin, M. D., Parren, P. W. H. I., Rudd, P. M., Dwek, R. A., Burton, D. R., and Wilson, I. A. (2002) Contrasting IgG Structures Reveal Extreme Asymmetry and Flexibility. *J. Mol. Biol.* 319, 9–18.
- (7) Marquart, M., Deisenhofer, J., Huber, R., and Palm, W. (1980) Crystallographic refinement and atomic models of the intact immunoglobulin molecule Kol and its antigen-binding fragment at 3.0 Å and 1.9 Å resolution. *J. Mol. Biol.* 141, 369–391.
- (8) Sandin, S., Öfverstedt, L.-G., Wikström, A.-C., Wrangé, Ö., and Sköglund, U. (2004) Structure and Flexibility of Individual Immunoglobulin G Molecules in Solution. *Structure* 12, 409–415.
- (9) Teilum, K., Olsen, J. G., and Kragelund, B. B. (2009) Functional aspects of protein flexibility. *Cell. Mol. Life Sci.* 66, 2231–2247.
- (10) Závodszky, P., Kardos, J., Svingor, Á., and Petsko, G. A. (1998) Adjustment of conformational flexibility is a key event in the thermal adaptation of proteins. *Proc. Natl. Acad. Sci. U.S.A.* 95, 7406–7411.
- (11) Eisenmesser, E. Z., Millet, O., Labeikovsky, W., Korzhnev, D. M., Wolf-Watz, M., Bosco, D. A., Skalicky, J. J., Kay, L. E., and Kern, D. (2005) Intrinsic dynamics of an enzyme underlies catalysis. *Nature* 438, 117–121.
- (12) Tang, K. E., and Dill, K. A. (1998) Native protein fluctuations: The conformational-motion temperature and the inverse correlation of protein flexibility with protein stability. *J. Biomol. Struct. Dyn.* 16, 397–411.



- (13) Vihinen, M. (1987) Relationship of protein flexibility to thermostability. *Protein Eng.* 1, 477–480.
- (14) Thakkar, S. V., Kim, J. H., Samra, H. S., Sathish, H. A., Bishop, S. M., Joshi, S. B., Volkin, D. B., and Middaugh, C. R. (2012) Local dynamics and their alteration by excipients modulate the global conformational stability of an IgG1 monoclonal antibody. *J. Pharm. Sci.* 101, 4444–4457.
- (15) Mahler, H.-C., Friess, W., Grauschopf, U., and Kiese, S. (2009) Protein aggregation: Pathways, induction factors and analysis. *J. Pharm. Sci.* 98, 2909–2934.
- (16) Tyagi, A. K., Randolph, T. W., Dong, A., Maloney, K. M., Hitscherich, C., and Carpenter, J. F. (2009) IgG particle formation during filling pump operation: A case study of heterogeneous nucleation on stainless steel nanoparticles. *J. Pharm. Sci.* 98, 94–104.
- (17) Harris, R. J., Shire, S. J., and Winter, C. (2004) Commercial manufacturing scale formulation and analytical characterization of therapeutic recombinant antibodies. *Drug Dev. Res.* 61, 137–154.
- (18) Mahler, H. C., Muller, R., Friess, W., Delille, A., and Matheus, S. (2005) Induction and analysis of aggregates in a liquid IgG1-antibody formulation. *Eur. J. Pharm. Biopharm.* 59, 407–417.
- (19) Roberts, C. J., Das, T. K., and Sahin, E. (2011) Predicting solution aggregation rates for therapeutic proteins: Approaches and challenges. *Int. J. Pharm.* 418, 318–333.
- (20) Wang, X., Das, T. K., Singh, S. K., and Kumar, S. (2009) Potential aggregation prone regions in biotherapeutics: A survey of commercial monoclonal antibodies. *mAbs* 1, 254–267.
- (21) Chennamsetty, N., Helk, B., Voynov, V., Kayser, V., and Trout, B. L. (2009) Aggregation-Prone Motifs in Human Immunoglobulin G. *J. Mol. Biol.* 391, 404–413.
- (22) Wang, W., Singh, S., Zeng, D. L., King, K., and Nema, S. (2007) Antibody structure, instability, and formulation. *J. Pharm. Sci.* 96, 1–26.
- (23) Kamerzell, T. J., Esfandiary, R., Joshi, S. B., Middaugh, C. R., and Volkin, D. B. (2011) Protein-excipient interactions: Mechanisms and biophysical characterization applied to protein formulation development. *Adv. Drug Delivery Rev.* 63, 1118–1159.
- (24) Hofmeister, F. (1888) Zur Lehre von der Wirkung der Salze, Naunyn-Schmiedeberg's. *Arch. Pharmacol.* 24, 247–260.
- (25) Baldwin, R. L. (1996) How Hofmeister ion interactions affect protein stability. *Biophys. J.* 71, 2056–2063.
- (26) Vonhippel, P. H., and Wong, K. Y. (1964) Neutral salts: The generality of their effects on the stability of macromolecular conformations. *Science* 145, 577–580.
- (27) Cohn, E. J., and Edsall, J. T. (1943) *Proteins, amino acids, and peptides as ions and dipolar ions*, Reinhold Publishing Corp., New York.
- (28) Nakagawa, T. (1995) Is viscosity B coefficient characteristic for solute-solvent interaction? *J. Mol. Liq.* 63, 303–316.
- (29) Broering, J. M., and Bommarius, A. S. (2005) Evaluation of Hofmeister Effects on the Kinetic Stability of Proteins. *J. Phys. Chem. B* 109, 20612–20619.
- (30) Von Hippel, P. H., and Schleich, T. (1969) Ion effects on the solution structure of biological macromolecules. *Acc. Chem. Res.* 2, 257–265.
- (31) Shukla, D., Schneider, C. P., and Trout, B. L. (2011) Complex Interactions between Molecular Ions in Solution and Their Effect on Protein Stability. *J. Am. Chem. Soc.* 133, 18713–18718.
- (32) Rubin, J., San Miguel, A., Bommarius, A. S., and Behrens, S. H. (2010) Correlating Aggregation Kinetics and Stationary Diffusion in Protein–Sodium Salt Systems Observed with Dynamic Light Scattering. *J. Phys. Chem. B* 114, 4383–4387.
- (33) Zhang-van Enk, J., Mason, B. D., Yu, L., Zhang, L., Hamouda, W., Huang, G., Liu, D., Remmele, R. L., and Zhang, J. (2012) Perturbation of Thermal Unfolding and Aggregation of Human IgG1 Fc Fragment by Hofmeister Anions. *Mol. Pharmacol.* 10, 619–630.
- (34) Zhang, Y., and Cremer, P. S. (2006) Interactions between macromolecules and ions: The Hofmeister series. *Curr. Opin. Chem. Biol.* 10, 658–663.
- (35) Parsons, D. F., Bostrom, M., Nostro, P. L., and Ninham, B. W. (2011) Hofmeister effects: Interplay of hydration, nonelectrostatic potentials, and ion size. *Phys. Chem. Chem. Phys.* 13, 12352–12367.
- (36) Gokarn, Y. R., Fesinmeyer, R. M., Saluja, A., Razinkov, V., Chase, S. F., Laue, T. M., and Brems, D. N. (2011) Effective charge measurements reveal selective and preferential accumulation of anions, but not cations, at the protein surface in dilute salt solutions. *Protein Sci.* 20, 580–587.
- (37) Arakawa, T., and Timasheff, S. N. (1982) Preferential interactions of proteins with salts in concentrated solutions. *Biochemistry* 21, 6545–6552.
- (38) Collins, K. D. (2012) Why continuum electrostatics theories cannot explain biological structure, polyelectrolytes or ionic strength effects in ion–protein interactions. *Biophys. Chem.* 167, 43–59.
- (39) Collins, K. D., and Washabaugh, M. W. (1985) The Hofmeister effect and the behaviour of water at interfaces. *Q. Rev. Biophys.* 18, 323–422.
- (40) Kamerzell, T. J., and Middaugh, C. R. (2008) The complex inter-relationships between protein flexibility and stability. *J. Pharm. Sci.* 97, 3494–3517.
- (41) Thakkar, S. V., Joshi, S. B., Jones, M. E., Sathish, H. A., Bishop, S. M., Volkin, D. B., and Middaugh, C. R. (2012) Excipients differentially influence the conformational stability and pretransition dynamics of two IgG1 monoclonal antibodies. *J. Pharm. Sci.* 101, 3062–3077.
- (42) Lilyestrom, W. G., Shire, S. J., and Scherer, T. M. (2012) Influence of the Cosolute Environment on IgG Solution Structure Analyzed by Small-Angle X-ray Scattering. *J. Phys. Chem. B* 116, 9611–9618.
- (43) Zhang, Z., and Smith, D. L. (1993) Determination of amide hydrogen exchange by mass spectrometry: A new tool for protein structure elucidation. *Protein Sci.* 2, 522–531.
- (44) Englander, S. W. (2006) Hydrogen Exchange and Mass Spectrometry: A Historical Perspective. *J. Am. Soc. Mass Spectrom.* 17, 1481–1489.
- (45) Houde, D., Berkowitz, S. A., and Engen, J. R. (2011) The utility of hydrogen/deuterium exchange mass spectrometry in biopharmaceutical comparability studies. *J. Pharm. Sci.* 100, 2071–2086.
- (46) Federici, M., Lubiniecki, A., Manikwar, P., and Volkin, D. B. (2012) Analytical lessons learned from selected therapeutic protein drug comparability studies. *Biologicals*, S1045-1056(12)00153-4.
- (47) Houde, D., Arndt, J., Domeier, W., Berkowitz, S., and Engen, J. R. (2009) Characterization of IgG1 Conformation and Conformational Dynamics by Hydrogen/Deuterium Exchange Mass Spectrometry. *Anal. Chem.* 81, 2644–2651.
- (48) Houde, D., Peng, Y., Berkowitz, S. A., and Engen, J. R. (2010) Post-translational Modifications Differentially Affect IgG1 Conformation and Receptor Binding. *Mol. Cell. Proteomics* 9, 1716–1728.
- (49) Burkitt, W., Domann, P., and O'Connor, G. (2010) Conformational changes in oxidatively stressed monoclonal antibodies studied by hydrogen exchange mass spectrometry. *Protein Sci.* 19, 826–835.
- (50) Tang, L., Sundaram, S., Zhang, J., Carlson, P., Matathia, A., Parekh, B., Zhou, Q., and Hsieh, M. C. (2013) Conformational characterization of the charge variants of a human IgG1 monoclonal antibody using H/D exchange mass spectrometry. *mAbs* 5, 114–125.
- (51) Zhang, A., Singh, S., Shirts, M., Kumar, S., and Fernandez, E. (2012) Distinct Aggregation Mechanisms of Monoclonal Antibody Under Thermal and Freeze-Thaw Stresses Revealed by Hydrogen Exchange. *Pharm. Res.* 29, 236–250.
- (52) Majumdar, R., Manikwar, P., Hickey, J. M., Arora, J., Middaugh, C. R., Volkin, D. B., and Weis, D. D. (2012) Minimizing Carry-Over in an Online Pepsin Digestion System used for the H/D Exchange Mass Spectrometric Analysis of an IgG1 Monoclonal Antibody. *J. Am. Soc. Mass Spectrom.* 23, 2140–2148.
- (53) Saphire, E. O., Parren, P. W. H. I., Pantophlet, R., Zwick, M. B., Morris, G. M., Rudd, P. M., Dwek, R. A., Stanfield, R. L., Burton, D. R., and Wilson, I. A. (2001) Crystal Structure of a Neutralizing Human IgG Against HIV-1: A Template for Vaccine Design. *Science* 293, 1155–1159.



- (54) Larkin, M. A., Blackshields, G., Brown, N. P., Chenna, R., McGettigan, P. A., McWilliam, H., Valentin, F., Wallace, I. M., Wilm, A., Lopez, R., Thompson, J. D., Gibson, T. J., and Higgins, D. G. (2007) Clustal W and Clustal X version 2.0. *Bioinformatics* 23, 2947–2948.
- (55) Vermeer, A. W., and Norde, W. (2000) The thermal stability of immunoglobulin: Unfolding and aggregation of a multi-domain protein. *Biophys. J.* 78, 394–404.
- (56) Vermeer, A. W., Norde, W., and van Amerongen, A. (2000) The unfolding/denaturation of immunoglobulin of isotype 2b and its F(ab) and F(c) fragments. *Biophys. J.* 79, 2150–2154.
- (57) Feige, M. J., Walter, S., and Buchner, J. (2004) Folding mechanism of the CH2 antibody domain. *J. Mol. Biol.* 344, 107–118.
- (58) Lilie, H., Jaenicke, R., and Buchner, J. (1995) Characterization of a quaternary-structured folding intermediate of an antibody Fab-fragment. *Protein Sci.* 4, 917–924.
- (59) Li, C. H., Narhi, L. O., Wen, J., Dimitrova, M., Wen, Z. Q., Li, J., Pollastrini, J., Nguyen, X., Tsuruda, T., and Jiang, Y. (2012) Effect of pH, Temperature, and Salt on the Stability of *Escherichia coli*- and Chinese Hamster Ovary Cell-Derived IgG1 Fc. *Biochemistry* 51, 10056–10065.
- (60) Bond, M. D., Panek, M. E., Zhang, Z., Wang, D., Mehndiratta, P., Zhao, H., Gunton, K., Ni, A., Nedved, M. L., Burman, S., and Volkin, D. B. (2010) Evaluation of a dual-wavelength size exclusion HPLC method with improved sensitivity to detect protein aggregates and its use to better characterize degradation pathways of an IgG1 monoclonal antibody. *J. Pharm. Sci.* 99, 2582–2597.
- (61) Bai, Y., Milne, J. S., Mayne, L., and Englander, S. W. (1993) Primary structure effects on peptide group hydrogen exchange. *Proteins: Struct., Funct., Bioinf.* 17, 75–86.
- (62) Milne, J. S., Mayne, L., Roder, H., Wand, A. J., and Englander, S. W. (1998) Determinants of protein hydrogen exchange studied in equine cytochrome c. *Protein Sci.* 7, 739–745.
- (63) Wang, F., Shi, W., Nieves, E., Angeletti, R. H., Schramm, V. L., and Grubmeyer, C. (2001) A transition-state analogue reduces protein dynamics in hypoxanthine-guanine phosphoribosyltransferase. *Biochemistry* 40, 8043–8054.
- (64) Bennett, B. C., Gardberg, A. S., Blair, M. D., and Dealwis, C. G. (2008) On the determinants of amide backbone exchange in proteins: A neutron crystallographic comparative study. *Acta Crystallogr. D* 64, 764–783.
- (65) Hvidt, A., and Linderstrom-Lang, K. (1954) Exchange of hydrogen atoms in insulin with deuterium atoms in aqueous solutions. *Biochim. Biophys. Acta* 14, 574–575.
- (66) Hvidt, A., and Nielsen, S. O. (1966) Hydrogen exchange in proteins. *Adv. Protein Chem.* 21, 287–386.
- (67) Kim, P. S., and Baldwin, R. L. (1982) Influence of charge on the rate of amide proton exchange. *Biochemistry* 21, 1–5.
- (68) Rohl, C. A., and Baldwin, R. L. (1997) Comparison of NH exchange and circular dichroism as techniques for measuring the parameters of the helix-coil transition in peptides. *Biochemistry* 36, 8435–8442.
- (69) Tadeo, X., Castano, D., and Millet, O. (2007) Anion modulation of the  $^1\text{H}/^2\text{H}$  exchange rates in backbone amide protons monitored by NMR spectroscopy. *Protein Sci.* 16, 2733–2740.
- (70) Zhang, A., Qi, W., Singh, S., and Fernandez, E. (2011) A New Approach to Explore the Impact of Freeze-Thaw Cycling on Protein Structure: Hydrogen/Deuterium Exchange Mass Spectrometry (HX-MS). *Pharm. Res.* 1–15.
- (71) Wang, L. C., Morgan, L. K., Godakumbura, P., Kenney, L. J., and Anand, G. S. (2012) The inner membrane histidine kinase EnvZ senses osmolality via helix-coil transitions in the cytoplasm. *EMBO J.* 31, 2648–2659.
- (72) Vrbka, L., Jungwirth, P., Bauduin, P., Touraud, D., and Kunz, W. (2006) Specific ion effects at protein surfaces: A molecular dynamics study of bovine pancreatic trypsin inhibitor and horseradish peroxidase in selected salt solutions. *J. Phys. Chem. B* 110, 7036–7043.
- (73) Fesinmeyer, R. M., Hogan, S., Saluja, A., Brych, S. R., Kras, E., Narhi, L. O., Brems, D. N., and Gokarn, Y. R. (2009) Effect of ions on agitation- and temperature-induced aggregation reactions of antibodies. *Pharm. Res.* 26, 903–913.
- (74) Ionescu, R. M., Vlasak, J., Price, C., and Kirchmeier, M. (2008) Contribution of variable domains to the stability of humanized IgG1 monoclonal antibodies. *J. Pharm. Sci.* 97, 1414–1426.
- (75) Faria, T. Q., Mingote, A., Siopa, F., Ventura, R., Maycock, C., and Santos, H. (2008) Design of new enzyme stabilizers inspired by glycosides of hyperthermophilic microorganisms. *Carbohydr. Res.* 343, 3025–3033.
- (76) Ramos, C. H. I., and Baldwin, R. L. (2002) Sulfate anion stabilization of native ribonuclease A both by anion binding and by the Hofmeister effect. *Protein Sci.* 11, 1771–1778.
- (77) Nishimura, C., Uversky, V. N., and Fink, A. L. (2001) Effect of salts on the stability and folding of staphylococcal nuclease. *Biochemistry* 40, 2113–2128.
- (78) Mason, P. E., Dempsey, C. E., Vrbka, L., Heyda, J., Brady, J. W., and Jungwirth, P. (2009) Specificity of Ion-Protein Interactions: Complementary and Competitive Effects of Tetrapropylammonium, Guanidinium, Sulfate, and Chloride Ions. *J. Phys. Chem. B* 113, 3227–3234.
- (79) Wernersson, E., Heyda, J., Kubickova, A., Krizek, T., Coufal, P., and Jungwirth, P. (2010) Effect of association with sulfate on the electrophoretic mobility of polyarginine and polylysine. *J. Phys. Chem. B* 114, 11934–11941.
- (80) Broide, M. L., Tominc, T. M., and Saxowsky, M. D. (1996) Using phase transitions to investigate the effect of salts on protein interactions. *Phys. Rev. E* 53, 6325–6335.
- (81) Arosio, P., Jaquet, B., Wu, H., and Morbidelli, M. (2012) On the role of salt type and concentration on the stability behavior of a monoclonal antibody solution. *Biophys. Chem.* 168–169, 19–27.
- (82) Weissenborn, P. K., and Pugh, R. J. (1996) Surface Tension of Aqueous Solutions of Electrolytes: Relationship with Ion Hydration, Oxygen Solubility, and Bubble Coalescence. *J. Colloid Interface Sci.* 184, 550–563.
- (83) Melander, W., and Horváth, C. (1977) Salt effects on hydrophobic interactions in precipitation and chromatography of proteins: An interpretation of the lyotropic series. *Arch. Biochem. Biophys.* 183, 200–215.
- (84) Foster, P. R., Dunnill, P., and Lilly, M. D. (1976) The kinetics of protein salting-out: Precipitation of yeast enzymes by ammonium sulfate. *Biotechnol. Bioeng.* 18, 545–580.
- (85) Pedersen, J. S., Flink, J. M., Dikov, D., and Otzen, D. E. (2006) Sulfates Dramatically Stabilize a Salt-Dependent Type of Glucagon Fibrils. *Biophys. J.* 90, 4181–4194.
- (86) Arakawa, T., and Timasheff, S. N. (1984) Mechanism of protein salting in and salting out by divalent cation salts: Balance between hydration and salt binding. *Biochemistry* 23, 5912–5923.
- (87) Washabaugh, M. W., and Collins, K. D. (1986) The systematic characterization by aqueous column chromatography of solutes which affect protein stability. *J. Biol. Chem.* 261, 12477–12485.
- (88) Ries-Kautt, M. M., and Ducruix, A. F. (1989) Relative effectiveness of various ions on the solubility and crystal growth of lysozyme. *J. Biol. Chem.* 264, 745–748.
- (89) Huang, H., Manciu, M., and Ruckenstein, E. (2005) On the Restabilization of Protein-Covered Latex Colloids at High Ionic Strengths. *Langmuir* 21, 94–99.
- (90) Gibb, C. L. D., and Gibb, B. C. (2011) Anion Binding to Hydrophobic Concavity Is Central to the Salting-in Effects of Hofmeister Chaotropes. *J. Am. Chem. Soc.* 133, 7344–7347.
- (91) Collins, K. D. (2004) Ions from the Hofmeister series and osmolytes: Effects on proteins in solution and in the crystallization process. *Methods* 34, 300–311.
- (92) Collins, K. D., Neilson, G. W., and Enderby, J. E. (2007) Ions in water: Characterizing the forces that control chemical processes and biological structure. *Biophys. Chem.* 128, 95–104.
- (93) Mason, B. D., Zhang-van Enk, J., Zhang, L., Remmele, R. L., and Zhang, J. (2010) Liquid-Liquid Phase Separation of a Monoclonal Antibody and Nonmonotonic Influence of Hofmeister Anions. *Biophys. J.* 99, 3792–3800.

- (94) Zhang, L., and Zhang, J. (2012) Specific ion-protein interactions dictate solubility behavior of a monoclonal antibody at low salt concentrations. *Mol. Pharmaceutics* 9, 2582–2590.
- (95) Zhang, L., Tan, H., Fesinmeyer, R. M., Li, C., Catrone, D., Le, D., Remmele, R. L., and Zhang, J. (2012) Antibody solubility behavior in monovalent salt solutions reveals specific anion effects at low ionic strength. *J. Pharm. Sci.* 101, 965–977.
- (96) Tobler, S. A., and Fernandez, E. J. (2002) Structural features of interferon- $\gamma$  aggregation revealed by hydrogen exchange. *Protein Sci.* 11, 1340–1352.
- (97) Manikwar, P., Majumdar, R., Hickey, J. M., Santosh, V. T., Samra, H. S., Sathish, H. A., Bishop, S. M., Middaugh, C. R., Volkin, D. B., and Weis, D. D. (2013) Pharmaceutical Excipient Effects on IgG1 Local Dynamics as Measured by Hydrogen-Deuterium Exchange Mass Spectrometry and Correlations with Physical and Storage Stability. *J. Pharm. Sci.*, DOI: 10.1002/jps.23543, [Epub ahead of print].
- (98) Zhang, J., and Topp, E. M. (2012) Protein G, Protein A and Protein A-Derived Peptides Inhibit the Agitation Induced Aggregation of IgG. *Mol. Pharmaceutics* 9, 622–628.
- (99) Gong, R., Vu, B. K., Feng, Y., Prieto, D. A., Dyba, M. A., Walsh, J. D., Prabakaran, P., Veenstra, T. D., Tarasov, S. G., Ishima, R., and Dimitrov, D. S. (2009) Engineered Human Antibody Constant Domains with Increased Stability. *J. Biol. Chem.* 284, 14203–14210.
- (100) Tomé, L. I. N., Jorge, M., Gomes, J. R. B., and Coutinho, J. o. A. P. (2010) Toward an Understanding of the Aqueous Solubility of Amino Acids in the Presence of Salts: A Molecular Dynamics Simulation Study. *J. Phys. Chem. B* 114, 16450–16459.
- (101) Shukla, D., and Trout, B. L. (2011) Preferential interaction coefficients of proteins in aqueous arginine solutions and their molecular origins. *J. Phys. Chem. B* 115, 1243–1253.
- (102) Shukla, D., Shinde, C., and Trout, B. L. (2009) Molecular computations of preferential interaction coefficients of proteins. *J. Phys. Chem. B* 113, 12546–12554.
- (103) Shukla, D., Schneider, C. P., and Trout, B. L. (2011) Molecular level insight into intra-solvent interaction effects on protein stability and aggregation. *Adv. Drug Delivery Rev.* 63, 1074–1085.